World Conference on Timber Engineering Oslo 2023

CYCLIC BEHAVIOR OF MORTISE-TENON JOINTS REINFORCED BY SELF-TAPPING SCREW

Tianxiao Yin[1], Chenyue Guo[2], Zhiqiang Wang[3,*], Wei Zheng[4], Jianhui Zhou[5], Meng Gong[6]

ABSTRACT: In this study, fully-thread countersunk head self-tapping screw (STS) with outer diameter of 6 mm and 8 mm were used to reinforce the mortise-tenon (MT) joints with horizontal and inclined insertion methods. A total of fifteen cyclic loading tests were carried out for one group of unreinforced joints and five groups of reinforced joints, and the load-carrying capacity, strength, stiffness, ductility and energy dissipation of these joints were evaluated. The results showed that larger diameter STS and more STS could improve the load-carrying capacity and initial stiffness of the joints, although it might accelerate the damage to the joints and change the failure modes of MT joints. In addition, different reinforcement methods had different improvement effect, as the joints reinforced by STS horizontal insertion had a more significant improvement in the load-carrying capacity, while the inclined insertion of STS had a more significant improvement in the initial stiffness. This study provides data for reinforcement of MT joints with STS, and different reinforcement methods can be selected according to different engineering requirements.

KEYWORDS: Timber, Mortise-tenon (MT) joint, Self-tapping screw (STS), Reinforcement, Cyclic loading

1 INTRODUCTION

As a kind of essential connection in Chinese traditional architecture, mortise-tenon (MT) joints are the main energy dissipation components in wood construction, which are easy to install and have good rotation ability [1]. Previous research found that MT joints belongs to semi-rigid joints [2,3]. With the development of modern timber construction, the bearing capacity and stiffness of traditional MT joints can hardly meet the engineering requirements. In order to improve the mechanical properties of MT joints, kinds of different reinforcement methods have been carried out for MT joints.

Currently, the reinforcement methods designed for MT joints can be categorized as three types according to the materials applied: wood component [4,5], metal connector [6-8] and new composite material component [9-11]. However, these methods have some shortcomings to some extent. For instance, the durability of wood components is not ideal, and the appearances of the MT joints reinforced by metal connectors (e.g. steel plate) and composite material (e.g. fiber reinforced polymer) are not clean and tidy. Thus, some new reinforcement methods need to be carried out.

Inspired by the connections in modern timber construction, some new dowel-type connectors can be considered for application in the reinforcement for MT joints. Among them, self-tapping screw (STS) is widely recognized as the state-of-the-art connector for timber construction, for its economic cost and convenient installation as well as its excellent mechanical properties [12-15]. According to former scholars' researches, carpentry joints reinforced by STS can achieve good performance, especially the stiffness and load-carrying capacity, which can compensate for the shortcomings of traditional MT joints [12-16]. Furthermore, previous researches found that the insertion angle of STS had a significant influence on the mechanical properties of those reinforced joints [14, 17-20]. At present, it is generally believed that the STS inserted perpendicular to the surface of the components can obtain better ductility, while STS inclined insertion can achieve better stiffness, both of which can improve the load-carrying capacity of the joints.

This paper presents glulam MT dovetail reinforced by STS with horizontal (perpendicular to the timber surface)

[1] Tianxiao Yin, College of Materials Science and Engineering, Nanjing Forestry University, China, yintianxiao@njfu.edu.cn
[2] Chenyue Guo, School of Engineering, University of Northern British Columbia, Canada, cguo@unbc.ca
[3] Zhiqiang Wang, College of Materials Science and Engineering, Nanjing Forestry University, China, wangzhiqiang@njfu.edu.cn
[4] Wei Zheng, College of Materials Science and Engineering, Nanjing Forestry University, China, zw@njfu.edu.cn
[5] Jianhui Zhou, School of Engineering, University of Northern British Columbia, Canada, jianhui.zhou@unbc.ca
[6] Meng Gong, Wood Science and Technology Centre, University of New Brunswick, Canada, meng.gong@unb.ca
* Corresponding author

https://doi.org/10.52202/069179-0155

and inclined insertion methods. Cyclic loading testes were carried in this study for both unreinforced (CG) and reinforced joints to evaluate their load-carrying capacity, strength, stiffness, ductility and energy dissipation capacity.

2 MATERIALS AND METHODS

2.1 MATERIALS

Four-layer Glulam made of NO.2 SPF (*Spruce-pine-fir*) dimension lumber were used for process of MT joints. The moisture content and density of glulam were 13.3% (COV=6.7%) and 449 kg/m^3 (COV=4.8%), respectively. Fully-thread countersunk head STS (grade 1022 [21]) with a diameter of 6 mm and 8 mm were used in this study. The yield moment ($M_{y,R}$) and the pull-through capacity (F_{head}) of STS were tested and evaluated respectively [22, 23], and the characteristic values were calculated [24], as shown in Table 1.

The dimension of the components was designed according to the Qing Dynasty " *Gong Cheng Zuo Fa Ze Li*" [25] and is shown in Fig. 1. The different reinforcement methods for MT joints are shown in Fig. 2. In order to ensure the uniformity of materials for specimens, the beam, column and crosser (a tamping placed in the groove of mortise upon tenon) used the same material and were assembled without adhesive.

Table 2 shows the grouping of specimens. It should be noted that in the preliminary tests, the tenon would split when the STS with 8mm diameter was applied for inclined insertion, so this diameter was not considered for use as inclined-insertion reinforcement for MT joints in the formal tests.

Table 1 *Properties of STS*

	Outer diameter d (mm)	Length l (mm)	$M_{y,R}$ (N·mm)	F_{head} (N)
STS-6	6	140	11090	3261
STS-8	8	140	34406	3927

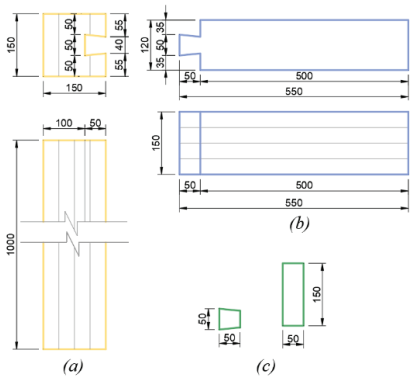

Figure 1: *Dimension of components in joints: (a) Column; (b) Beam and (c) Crosser (Unit: mm).*

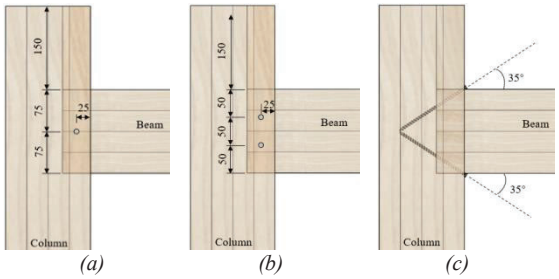

Figure 2: *different reinforcement methods: (a) one STS with horizontal insertion, (b) two STS with horizontal insertion and (c) two STS with inclined insertion.*

Table 2 *Specimen grouping*

Group	Number of STS	Diameter of STS (mm)	Insertion angle (°)	Replicates
CG	/	/	/	3
RSV6	1	6	90°	3
RSV8	1	8	90°	3
RV6	2	6	90°	3
RV8	2	8	90°	3
RI6	1	6	35°	3

2.2 TEST SETUP

During tests, the columns were placed horizontally and horizontal force was acted on the beam end by hydraulic actuator. The rightward push was recorded as positive direction and the leftward pull was recorded as negative direction. Approximately 10 kN horizontal load was applied at the end of the column through a hydraulic jack to simulate the load of the column under actual situation. The whole test setup is shown in Fig.3. The loading protocol referred to ISO-16670 [26]. The cyclic loading tests were repeated three times for each group.

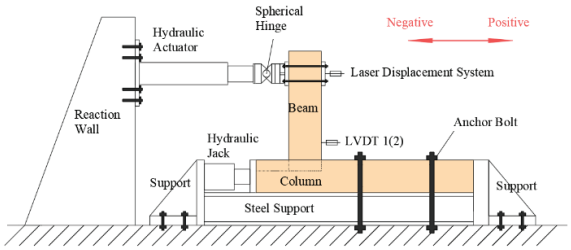

Figure 3: *Test setup.*

2.3 DATA ANALYSIS

The bending moment (M) and the corresponding rotation (θ) in this study were calculated by geometric relations as:

$$M = P \cdot H \quad (1)$$

$$\theta = \frac{\Delta}{H} \quad (2)$$

where P is the load applied, H is the distance between the joint and loading point (400 mm in this study), Δ is the displacement of the loading point in horizontal direction. The yield moment (M_y) of these joints was determined according to EEEP method [27] as:

$$M_y = (\theta_u - \sqrt{\theta_u^2 - \frac{2A}{K_e}})K_e \quad (3)$$

where M_y is the yield moment, θ_u is the ultimate rotation angle, A is the integral area under envelop curve in the interval of [0, θ_u], K_e is the initial stiffness which equals to 0.4 M_m/θ_e, where M_m is the maximum bending moment and θ_e is the rotation angle at 0.4 M_m.

Strength degradation factor (λ) was used to characterize the behavior that the strength of the joints decreases as the number of cycles increases [10], which was calculated as:

$$\lambda_i = \frac{M_{i,3}}{M_{i,1}} \quad (4)$$

where λ_i is the strength degradation factor in the i th displacement amplitude, $M_{i,1}/M_{i,3}$ is the peak bending moment of the first cycle in the i th displacement amplitude.

Stiffness degradation of joints was referred to evaluate the stiffness decreases in this study [28]. The secant stiffness K_i was calculated as:

$$K_i = \frac{|+M_i|+|-M_i|}{|+\theta_i|+|-\theta_i|} \quad (5)$$

where M_i is the peak bending moment of joints at the 1st cycle in the i-stage displacement amplitude while θ_i is the relevant rotation angle of M_i.

The ductility coefficient (D) of the joints in this study was evaluated as the ratio between the ultimate rotation (θ_u) and yield rotation (θ_m):

$$D = \frac{\theta_u}{\theta_y} \quad (6)$$

The ductility of joints into four scopes from brittle ($D \leq 2$) to high ductility ($D > 6$) according to their ductility coefficient [29].

The equivalent viscous damping coefficient (v_{ep}), which is a dimensionless coefficient, can be employed to assess the energy dissipation capacity of these joints [30]. The calculation of the equivalent viscous damping coefficient is as follows:

$$v_{ep} = \frac{E_d}{2\pi E_p} \quad (7)$$

where E_d is the energy dissipated per half cycle, E_p is the available potential energy.

3 RESULTS AND DISCUSSIONS

3.1 FAILURE MODES

The typical failure modes of the CG group were push out of crosser and pull-out of the tenon, together with splitting and crack on the column, as shown in Fig. 4.

As regards to the reinforced groups with STS horizontal insertion, split of the column and yielding of STS were the typical failure modes. Apart from this, the crack and crush of wood on the column below the joints area were also observed in these groups. For RSV6 and RSV8 groups reinforced with one STS, they had similar failure modes during the tests, which were the pull-out of the tenon and splitting on the side of the column, together with the yielding of STS, as shown in Fig. 5 and Fig. 6. Due to the larger diameter of STS, the amount of the pull-out of tenon in RSV6 group was larger than that in RSV8 group. The phenomenon of RV6 and RV8 groups during the initial loading phase was similar to RSV6 and RSV8 groups. Benefitted from the more rigid connection provided by two STS, the amount of tenon pull-out was decreased, compared with that in RSV6 and RSV8 groups. However, on account of the more STS inserted, the joints might suffer more damage at the late loading stage, for example, the column would split or even fracture. The two STS inserted in RV groups were yielded at the late loading stage. Typical failure modes of RV6 and RV8 are shown in Fig. 7 and Fig.8.

Similar to other groups, the pull-out of tenon and crack on the column appeared in RI6 group with STS inclined insertion. However, the difference between RI6 group and other groups was that there was no split on the side of the column in RI6 group and the STS used in it was not found yielding. After cutting the specimens, the withdrawal of STS was found in the RI6 group. The failure mode of RI6 group was shown in Fig. 9.

(a) (b) (c)

Figure 4: *Failure modes of CG group: (a) push-out of crosser; (b) pull-out of tenon and splitting on the side of column and (c) crack on the lower end of mortise of column.*

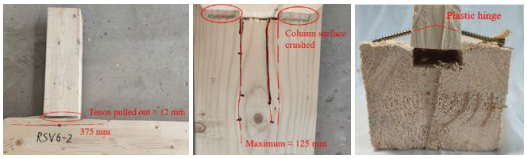

(a) (b) (c)

Figure 5: *Failure modes of RSV6 group: (a) pull-out of tenon and splitting on the side of column; (b) crack on the lower end of mortise of column and crush of wood and (c) STS yielding.*

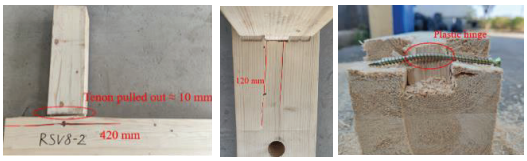

(a) (b) (c)

Figure 6: *Failure modes of RSV8 group: (a) pull-out of tenon and splitting on the side of column; (b) crack on the lower end of mortise of column and crush of wood and (c) STS yielding.*

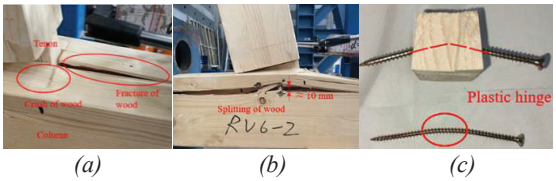

(a) (b) (c)

Figure 7: *Failure modes of RV6 group: (a) crush and fracture of wood; (b) splitting of wood and (c) STS yielding.*

https://doi.org/10.52202/069179-0155

(a) (b) (c)

Figure 8: *Failure modes of RV8 group: (a) crack, crush and fracture of wood; (b) splitting of wood and (c) STS yielding.*

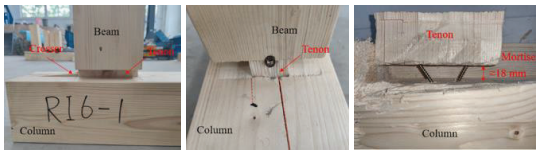

(a) (b) (c)

Figure 9: *Failure modes of RI6 group: (a) pull-out of tenon and crosser; (b) crack on the column and (c) withdrawal of STS.*

3.2 HYSTERETIC AND ENVELOP CURVES

The average hysteretic curves of each group showed different degree of pinching effect and exhibited asymmetry in positive and negative directions, as shown in Fig. 10.

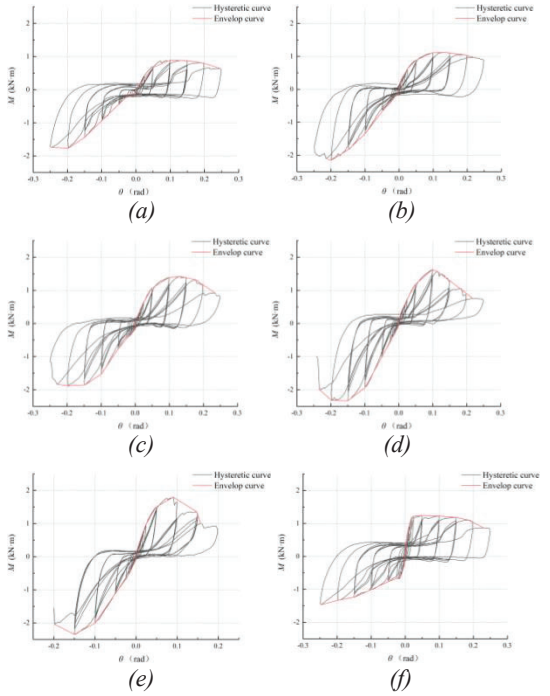

(a) (b) (c) (d) (e) (f)

Figure 10: *Hysteretic curves of: (a) CG group; (b) RSV6 group; (c)RSV8 group; (d) RV6 group; (e) RV8 group and (f) RI6 group.*

These hysteretic curves showed a similar trend. To be specific, the slope of hysteretic curve was small at the initial loading stage because of the processing gap between mortise and tenon. As the increment of displacement amplitude, the friction area between mortise and tenon increased thus caused the rapid increase of the bending moment. It can be obviously seen that the hysteretic curves of each joint have asymmetry, and the absolute value of the peak point of the negative loading curve was higher than that of the positive loading curve, which indicated that the negative loading process had a higher load-carrying capacity. The reason for this was the tenon was constrained differently under these loading directions. Specifically, under positive loading, the pushing out and loosening of the crosser would lead to a decrease in the load-carrying capacity, on the contrary, the rigid constraint had a positive effect on the improvement of the load-carrying capacity under negative loading tests. Different from the curves of the joints with horizontally inserted STS, the hysteretic curve of RI6 group exhibited excellent initial slope and alleviate pinching effect.

For easy comparison, the envelop curves of each group have been extracted and drawn in Fig. 11. It is clear from this figure that the RV groups had the largest load-carrying capacity, followed by the RSV groups and the RI6 group. In a homogeneous group, it can be found that a bigger diameter could provide higher load-carrying capacity. For example, as regard the RV groups, the RV8 group had a higher maximum bending moment than that of RV6 group. In general, the joints reinforced with STS horizontal insertion had significant improvement in terms to load-carrying capacity, while those with STS inclined insertion had obvious improvement in initial stiffness.

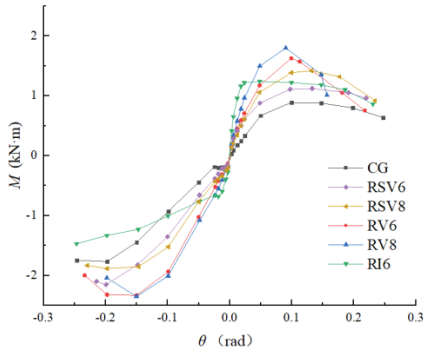

Figure 11: *Envelop curves of each group.*

3.3 MECHANICAL PROPERTIES

The average maximum moment (M_m), ultimate moment (M_u), yield moment (My) and their corresponding rotation together with the initial stiffness (K_e) and ductility coefficient (D) during two loading directions of each group are summarized in Table 3.

The load-carrying capacity and stiffness of MT joints have been improved significantly after being reinforced by STS. Two STS with horizontal insertion (RV group) had obvious improvement in load-carrying capacity, and STS with larger diameter had more improvement. Compared with the CG group, the load-carrying capacity of the RV group joints was 102% and 33% higher in positive and negative loading directions, respectively. As mentioned above, a larger diameter of STS can improve the load-carrying capacity due to its larger bending strength. Moreover, compared with RV groups and RSV groups, it can be concluded that the number of STS had a significant

https://doi.org/10.52202/069179-0155

effect on the load-carrying capacity of MT joints, although it did not meet a liner rule. From the results, it can be seen that the improvements of load-carrying capacity brought by RSV groups were not as good as that brought by RV groups. For instance, the maximum bending moment of the RSV8 and RSV6 groups increased by 59 % and 26%, respectively, which was smaller than the improvement of MT joints in RV groups. Furthermore, the reinforcement effect of RI6 group was small, under positive loading, the load-carrying capacity of MT joints was increased by 39%, while under negative loading, the load-carrying capacity of which was close to that of CG group. This means for this kind of MT joints, using horizontally inserted STS can achieve a higher improvement on load-carrying capacity

Table 3 *Mechanical properties of MT joints*

Group	Loading direction	M_m (kN·m)	θ_m (rad)	M_u (kN·m)	θ_u (rad)	M_y (kN·m)	θ_y (rad)	K_e (kN·m·rad^{-1})	D
CG	Positive	0.89	0.10	0.71	0.22	0.83	0.06	13.21	3.56
RSV6		1.12	0.13	0.96	0.22	1.03	0.03	29.97	6.43
RSV8		1.42	0.13	1.14	0.20	1.29	0.05	27.05	4.26
RV6		1.63	0.10	1.30	0.15	1.42	0.05	31.01	3.22
RV8		1.80	0.09	1.44	0.14	1.57	0.03	45.00	3.92
RI6		1.24	0.05	1.00	0.21	1.18	0.01	124.40	21.76
CG	Negative	1.77	0.20	1.74	0.25	1.83	0.20	9.18	1.23
RSV6		2.15	0.20	2.10	0.21	1.99	0.15	13.45	1.45
RSV8		1.88	0.20	1.83	0.23	1.86	0.12	15.38	1.90
RV6		2.33	0.15	2.00	0.23	2.19	0.11	20.73	2.21
RV8		2.35	0.15	2.04	0.20	2.13	0.09	23.48	2.19
RI6		1.47	0.25	1.47	0.25	1.11	0.02	48.93	10.91

compared with inclined insertion STS.

The strength degradation of each group between -0.15 rad to 0.15 rad is shown in Fig. 12. It can be easily seen that the strength degradation factor of each group decreased with the increase of loading amplitude. The strength degradation of CG group was more minor before rotation reached 0.15 rad, which may prove that the wood damage inside the unreinforced joints was slighter. Afterward, the strength of CG group degraded greatly due to the significant increase of tenon pulling out. It is worth noting that the strength degradation of RV groups was more prominent in this test, verifying that those joints suffered more damage in loading. On the contrary, the strength degradation of RSV and RI groups tended to be stable at the late loading stage.

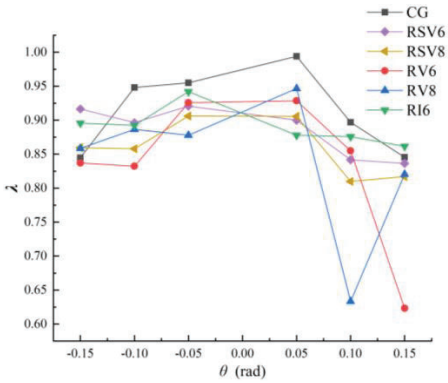

Figure 12: *Strength degradation of each group.*

The stiffness degradation of each group is shown in Fig. 13. In general, the stiffness of each group showed similarity before the rotation came to 0.05 rad, which decreased and then remained stable. When the rotation came to 0.25 rad, each group exhibited similar stiffness in the end, indicating that significant failure had occurred in each group. During the whole loading process, the unreinforced CG group showed a markedly lower stiffness than those of the reinforced group. In the reinforced groups, RI6 group exhibited very large stiffness in the initial loading stage, which could significantly improve the initial stiffness of MT joints, up to 842% and 433% higher than those of CG group, respectively in two loading directions. Comparing the RV groups with RSV groups, it can be found that MT joints reinforced with two STS can obtain higher initial stiffness than that of those reinforced with one STS. Besides, a bigger diameter of STS can also effectively improve the initial stiffness.

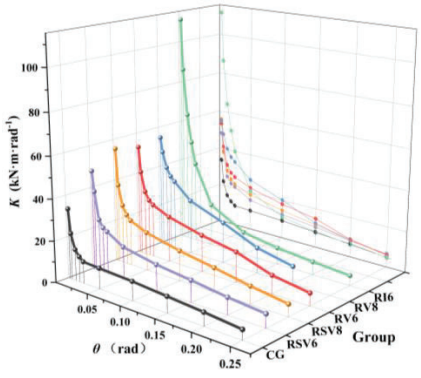

Figure 13: *Stiffness degradation of each group.*

As shown in Table 3, the ductility coefficient (D) of each group under positive loading was higher than that under negative loading. The reason for this was that the joints entered yield stage earlier when they were loaded in positive direction, due to the different constraints under

https://doi.org/10.52202/069179-0155

the two loading directions. It is worth noting that under positive loading, RSV groups had higher ductility coefficient than RV group, while under negative loading the situation was the opposite. The reason for this could be that, as mentioned, the constraints under negative loading were more rigid, thus leading to plastic deformation of wood in RV groups. As a result, RV groups entered the yield stage earlier, which makes the calculation result of ductility coefficient larger. Among these groups, the ductility of RI6 was significantly higher than that of other groups, while the ductility of CG group without reinforcement was relatively lower. According to the classification of ductility proposed by Smith et al. [29], except the RI6 group belongs to high ductility, other groups were classified as low ductility.

The equivalent viscous damping ratios curves of each group during tests are shown in Fig. 14. These joints exhibited similar energy dissipation trend during the whole loading test. To be specific, the energy dissipation capacity was low when the rotation was about 0 rad, before or after that, the energy dissipation capacity reached a high level. Combined with the damage of wood, it is easy to understand that when the rotation angle was about 0 rad, the joints were loose due to the repeated extrusion, leading to a low friction effect. As the displacement amplitude increased, the joints got close contact with surrounding components, the friction effect was enhanced, so the energy dissipation capacity increased. As regards reinforced groups, since joints experienced different extent of damage during loading process, the energy dissipation capacity has not got obvious improvement at late loading stage. On the contrary, CG group showed a stable energy dissipation during tests, and at late loading stage, its energy dissipation capacity was better than that of reinforced groups, even though its cumulative energy dissipation was not as good as others'. Among reinforced groups, RI6 group had the best energy dissipation capacity, especially when the rotation was not large. It can be considered that the friction between the thread of STS and wood hole contributed a lot to the energy dissipation. Generally speaking, the factors that influence the energy dissipation capacity of MT joints were friction and fracture of wood. In this study, the initial energy dissipation of joints depended mostly on the friction between mortise, tenon and STS, as loading continued, the damage of wood could absorb part of the energy, meanwhile, the joints began to loosen.

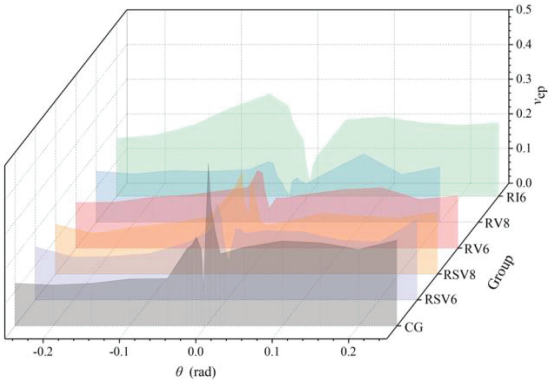

Figure 14: *Equivalent viscous damping ratios of each group.*

4 CONCLUSIONS

The MT joints reinforced by STS with different insertion methods could obtain an improvement on connection performance. Below are some conclusions summarized from this study:

(1) The typical failure modes of the unreinforced joints were the pull-put of tenon and the split on the column. Regarding the reinforced joints, the application of STS could significantly lower the pull-out amount of the tenon, especially when STS were inserted horizontally. On the other hand, the insertion of STS could also accelerate the damage of wood.

(2) Using more STS or increasing the diameter of STS could effectively improve the load-carrying capacity of MT joints, although this might hasten their failure.

(3) Inclined insertion of STS could help the MT joints obtain higher initial stiffness, stable strength degradation and better ductility and energy dissipation capacity.

(4) Further study about the configuration of MT joints and effect of the type of STS are worth conducting.

ACKNOWLEDGEMENT

This work was financially supported by the National Natural Science Foundation of China (Grant No. 32071700), the National Key Research and Development Program of China (Grant No. 2021YFD2200605) and Qing Lan Project.

REFERENCES

[1] P. Yu, Q. Yang, S. Law, Lateral behavior of heritage timber frames with loose nonlinear mortise-tenon connections, Structures. 33(2021) 581-592. DOI: 10.1016/j.istruc.2021.04.061.

[2] D.P. Fang, M.H. Yu, Y. Miyamoto, S. Iwasaki, H. Hikosaka.: Numerical analysis on structural characteristics of ancient timber architecture. Eng. Mech., 18 (1): 137-144, 2001.

[3] D.P. Fang, M.H. Yu, Y. Miyamoto, S. Iwasaki, H. Hikosaka, Experimental studies on structural

characteristics of ancient timber architectures, Eng. Mech. 17 (2) (2000) 75-83.
[4] L. B. Sandberg, W. M. Bulleit, E. H. Reid, Strength and stiffness of oak pegs in traditional timber-frame joints, J. Struct. Eng. 126 (6) (2000) 717-723. DOI: 10.1061/(ASCE)0733-9445(2000)126:6(717).
[5] T. Shiratori, K. Komatsu, A. Leijten, Modified traditional Japanese timber joint system with retrofitting abilities, Struct. Control Health Monit. 15 (7) (2008) 1036-1056. DOI: 10.1002/stc.240.
[6] Q. Zhou, W. Yan, Z. Li, B. Zhang, Experiments on the aseismic behavior of Chinese ancient architecture mortise-and-tenon joints strengthened with iron-hooks, Sci. Conserv. Archaeol. 23 (4) (2011) 17-25. DOI: 10.16334/j.cnki.cn31-1652/k.2011.04.002. [In Chinese].
[7] W. Lu, W. Sun, J. Gu, D. Deng, W. Liu, Experimental study on seismic performance of timber frames strengthened with curved steel dampers, J. Build. Struct. 35 (11) (2014) 151-157. DOI: 10.14006/j.jzjgxb.2014.11.019. [In Chinese].
[8] J. Xue, L. Zhai, F. Zhang, Y. Li, Performance analysis and design recommendations for damaged mortise-tenon joints of ancient timber structure strengthened with flat steel, J. Xi'an Univ. of Arch.& Tech. (Natural Science Edition). 47 (5) (2015) 621-625. DOI: 10.15986/j.1006-7930.2015.05.002. [In Chinese].
[9] K. U. Schober, A. M. Harte, R. Kliger, R. Jockwer, Q. Xu, J.F. Chen, FRP reinforcement of timber structures, Constr. Build. Mater. 97 (2015) 106-118. DOI: 10.1016/j.conbuildmat.2015.06.020.
[10] J. Xue, C. Wu, X. Zhang, Y. Zhang, Experimental study on seismic behavior of mortise-tenon joints reinforced with shape memory alloy, Eng. Struct. 218 (2020) 110839. DOI: 10.1016/j.engstruct.2020.110839.
[11] J. Xue, C. Wu, X. Zhang, Y. Zhang, Effect of pre-tension in superelastic shape memory alloy on cyclic behavior of reinforced mortise-tenon joints, Constr. Build. Mater. 241 (2020) 118136. DOI: 10.1016/j.conbuildmat.2020.118136.
[12] P. Dietsch, R. Brandner, Self-tapping screws and threaded rods as reinforcement for structural timber elements-A state-of-the-art report, Constr. Build. Mater. 97 (2015) 78-89. DOI: 10.1016/j.conbuildmat.2015.04.028.
[13] C. Zhang, H.B. Guo, K. Jung, R. Harris, W.S. Chang, Using self-tapping screw to reinforce dowel-type connection in a timber portal frame, Eng. Struct. 178 (2019) 656-664. DOI: 10.1016/j.engstruct.2018.10.066.
[14] T. Tannert, F. Lam, Self-tapping screws as reinforcement for rounded dovetail connections, Struct. Control Health Monit. 16 (3) (2009) 374-384. DOI: 10.1002/stc.283.
[15] X. Song, K. Li, E. Crayssac, Y. Wu, Lateral performance of traditional heavy timber frames with mortise-tenon joints retrofitted using self-tapping screws, J. Struct. Eng. 144 (10) (2018) 04018187. DOI: 10.1061/(ASCE)ST.1943-541X.0002191.
[16] H. Li, F. Lam, H. Qiu, Comparison of glulam beam-to-beam connections with round dovetail and half-lap joints reinforced with self-tapping screws, Constr. Build. Mater. 227 (2019) 116437. DOI: 10.1016/j.conbuildmat.2019.07.163.
[17] C. Loss, A. Hossain, T. Tannert, Simple cross-laminated timber shear connections with spatially arranged screws, Eng. Struct. 173 (2018) 340-356. DOI: 10.1016/j.engstruct.2018.07.004.
[18] J. R. Brown, M. Li, T. Tannert, D. Moroder, Experimental study on orthogonal joints in cross-laminated timber with self-tapping screws installed with mixed angles, Eng. Struct. 228 (2021) 111560. DOI: 10.1016/j.engstruct.2020.111560.
[19] D. Hanna, T. Tannert, Glulam connections assembled with screws in different installation angles, Maderas-Cienc. Tecnol. 23 (54) (2021) 1-14. DOI: 10.4067/s0718-221x2021000100454.
[20] A. Hossain, M. Popovski, T. Tannert, Cross-laminated timber connections assembled with a combination of screws in withdrawal and screws in shear, Eng. Struct. 168 (2018) 1-11. DOI: 10.1016/j.engstruct.2018.04.052.
[21] ASTM A29/A29M, Standard specification for general requirements for steel bars, carbon and alloy, hot-wrought, ASTM Standards, West Conshohocken, PA, USA, 2015.
[22] ASTM F1575, Standard test method for determining bending yield moment of nails, ASTM Standards, West Conshohocken, PA, USA, 2017.
[23] EN 1383:2016, Timber structures-Test methods-Pull through resistance of timber fasteners, European Committee for Standardization (CEN), Bruxelles, Belgium, 2016.
[24] EN 14358:2016, Timber structures-Calculation and verification of characteristic values, European Committee for Standardization, Bruxelles, Belgium, 2016.
[25] S. Liang, Illustration of Gong Cheng Zuo Fa Ze Li, Tsinghua University Press, Beijing, China, 2006. [In Chinese].
[26] ISO 16670: 2003, Timber structures-Joints made with mechanical fasteners-Quasi-static reversed-cyclic test method, Technical Committee ISO/TC 165, Timber structure, Ottawa, Canada, 2003.
[27] ASTM E2126, Standard test method for cyclic (reversed) load test for shear resistance of walls for buildings, ASTM Standards, West Conshohocken, PA, USA, 2005.
[28] JGJ/T 101-2015, Specification of test methods for earthquake resistant building, Ministry of Housing and Urban-Rural Development of the People's Republic of China, China Architecture & Building Press, Beijing, China, 2015. [In Chinese].
[29] I. Smith, A. Asiz, M. Snow, I. Chui, Possible Canadian/ISO approach to deriving design values from test data, The 39th CIB Working Commission W18-Timber Structures, Florence, Italy, August 2006.
[30] EN12512:2001, Timber structures-Test methods-Cyclic testing of joints made with mechanical fasteners, European Committee for Standardization, Bruxelles, Belgium, 2001.

https://doi.org/10.52202/069179-0155